Force balance of opposing diffusive motors generates polarity-sorted microtubule patterns

Clothilde Utzschneider[1]*, Bhagyanath Suresh[2]*, Alfredo Sciortino[2]*, Jérémie Gaillard[1], Alexandre Schaeffer[2], Sudipta Pattanayak[3], Jean-François Joanny[3,4#], Laurent Blanchoin[1,2#], Manuel Théry[1,2#]

1- CytoMorpho Lab, LPCV, UMR5168, Université Grenoble-Alpes, CEA/INRA/CNRS, Interdisciplinary Research Institute of Grenoble, 17 rue des Martyrs, 38054 Grenoble, France.
2- CytoMorpho Lab, CBI, UMR8132, Université Paris Sciences et Lettres, Ecole Supérieure de Physique et Chimie Industrielles de la Ville de Paris, CEA/CNRS, Institut Pierre Gilles De Gennes, 6 rue Jean Calvin, 75005, Paris France.
3- Collège de France, Université Paris Sciences et Lettres, 11 place Marcelin Berthelot, 75231 Paris, France.
4- Institut Curie, Université Paris Sciences et Lettres, Physique de la Cellule et cancer, UMR 168, 26 rue d'Ulm 74248 Paris Cedex 05, France

* These authors contributed equally to this work
# correspondence should be addressed to: jean-francois.joanny@college-de-france.fr, laurent.blanchoin@cnrs.fr, manuel.thery@cea.fr

Supplementary information

Materials and Methods

Protein expression, purification and labelling

Tubulin

Bovine brain tubulin was purified in BRB80 buffer (80 mM 1,4- piperazinediethanesulfonic acid, pH 6.8, 1 mM ethylene glycol tetraacetic acid, and 1 mM MgCl2) according to previously published method (*1*). Tubulin was purified from fresh bovine brain by three cycles of temperature-dependent assembly and disassembly in BRB80 supplemented with 1 mM GTP (*2*). MAP-free neurotubulin was purified using cation-exchange chromatography (EMD SO, 650 M, Merck) in 50 mM PIPES, pH 6.8, supplemented with 1 mM MgCl2, and 1 mM EGTA. Purified tubulin was obtained after a cycle of polymerization and depolymerization. Fluorescent tubulin (ATTO 488–labeled tubulin and ATTO 565–labeled tubulin) and biotinylated tubulin were prepared according to previously published method (*3*). Microtubules from neurotubulin were polymerized at 37°C for 30 min and layered onto cushions of 0.1 M NaHEPES, pH 8.6, 1 mM MgCl2, 1 mM EGTA, 60% v/v glycerol, and sedimented by high centrifugation at 30°C. Then microtubules were resuspended in 0.1 M NaHEPES pH 8.6, 1 mM MgCl2, 1 mM EGTA, 40% v/v glycerol and labeled by adding 1/10 volume 100 mM NHS-ATTO (ATTO Tec) for 10 min at 37°C. The labeling reaction was stopped using 2 volumes of 2X BRB80, containing 100 mM potassium glutamate and 40% v/v glycerol, and then microtubules were sedimented onto cushions of BRB80 supplemented with 60% glycerol. Microtubules were resuspended in cold BRB80. Microtubules were then depolymerised and a second cycle of polymerization and depolymerization was performed. Tubulin was kept in liquid nitrogen. Our labelling ratio is: for tubulin 488 nm 1.6 to 1.8 fluorophore per dimer, and for tubulin 565 nm 0.6 to 0.7 fluorophore per dimer. We used NanoDrop one UV-Vis spectrophotometer (Thermofisher) to determine the labelling efficiency.

NCD

Recombinant, truncated NCD motor protein (amino acid 236-700, accession number A0A0B4LI25) was purified using bacterial expression as previously described (*4*). The construct includes sequences encoding a His6 tag and GFP at the N-terminal end of the protein sequence. Expression of the plasmid, pET17b_NCD_GFP_His (24507, Addgene, Cambridge, MA) was induced by transfection into Rosetta2 (DE3)-pLysS E. coli (VWR), followed by induction with 0.2 mM IPTG for 16 h at 18°C.

The purification of the expressed kinesin was performed in three steps. First, the raw lysate was loaded onto a Ni-NTA column to affinity purify via the N-terminal histidine tag. The flow-through from this column was then slightly diluted and loaded onto an anion exchange column. The final purification step involved gel filtration. The motors were stored frozen at -80°C.

Procedure for Ni-NTA column purification: The pellet was lysed in 80 ml of lysis buffer (50 mM NaPO4, pH 8.0, 20 mM imidazole, 250 mM NaCl, 1 mM MgCl2, 0.5 mM ATP, 10 mM β-mercaproethanol, 1x protease inhibitor cocktail (complete, EDTA free, Roche, Mannheim, Germany)) and centrifuged at 25000g for 30 min at 4°C. The supernatant (lysate) was loaded onto a Ni-NTA column (HisTrap HP™, 17-5247-01, Cytiva), washed with washing buffer (50 mM NaPO4, pH 6.0, 250 mM NaCl, 1 mM MgCl2, 0.1 mM ATP, 10 mM β-mercaproethanol), and eluted with elution buffer (50 mM NaPO4, pH 7.2, 500 mM Imidazole, 250 mM NaCl, 1 mM MgCl2, 0.1 mM ATP, 10 mM β-mercaproethanol).

Procedure for the gel filtration column: The eluate from the anion exchange column was loaded onto an gel filtration column (hiload 16 600 superdex 200 pg, 28-9893-35, Cytiva) and eluted with NCD buffer (10 mM NaPO4, pH 7.2, 50 mM NaCl, 2 mM MgCl2, 1 mM EGTA, 1 mM DTT, 0.1 mM ATP).

KIF5B

Recombinant, truncated kinesin-1 motor protein (amino acids 1–560, accession number : P33176) was purified using bacterial expression as previously described (5). The construct includes the sequences encoding a His6 tag and SNAP tag at the C-terminal end of the protein sequence. The plasmid for the kinesin construct, pET17_K560_SNAP_His, was generously provided by Dr. Ross. The plasmid was introduced into Rosetta2 (DE3)-pLysS E. coli (VWR) by transformation, and induction was carried out with 0.2 mM IPTG for 16 hours at 18°C.

The purification of the expressed kinesin was performed in three steps. The first step involves using a cation exchange column. The bacteria pellet was lysed in 80 ml lysis buffer (Lysis buffer is a cation exchange buffer (6.7 mM sodium acetate, 6.7 mM 4-(2-hydroxyethyl)-1-piperazineethanesulfonic acid (HEPES), 6.7 mM 2-ethanesulfonic acid (MES), pH 7.0, 20 mM beta mercaptoethanol (BME), 0.2 mM ATP, 0.2% (w/v) polyoxyethylene (20) sorbitan monolaurate (TWEEN20)) supplemented with 1x protease inhibitor cocktail (complete, EDTA free, Roche, Mannheim, Germany) and TWEEN20 to a final concentration of 0.5% (w/v)). After sonication, and centrifugation at 25,000 g for 30 minutes at 4°C, the supernatant (lysate) was loaded onto a cation exchange column (HiTrap SP HP™, 17-1151-01, Cytiva), washed with washing buffer (cation exchange buffer supplemented with KCl to a final concentration of 50 mM) and eluted with elution buffer (cation exchange buffer supplemented with KCl to a final concentration of 300 mM).

The flow-through from that column was diluted 5-fold in nickel loading buffer (nickel buffer: 50 mM sodium phosphate buffer, pH 7.5, 5% w/v glycerol, 300 mM KCl, 1 mM MgCl2, 0.2% w/v TWEEN20, 10 mM BME, 0.1 mM ATP, supplemented with imidazole to a final concentration of 36 mM) and loaded onto a Ni-NTA column (HisTrap HP™, 17-5247-01, Cytiva), washed with nickel washing buffer (nickel buffer supplemented with KCl to a final concentration of 1000 mM and imidazole to a final concentration of 30 mM) and eluted with nickel elution buffer (nickel buffer supplemented with imidazole to a final concentration of 300 mM). We added SNAP surface Alexa Fluor 647 (S9136,New England Biolabs) at the same concentration as kinesin. The SNAP tag was labeled overnight at 4°C.

Fluorescently-labeled kinesin was loaded onto an gel filtration column (Superdex 200 Increase 10/300 GL, 28-9909-44, Cytiva) and eluted with K560 buffer (50 mM NaPO4 (pH7.4), 300 mM KCl, 1 mM MgCl2, 5% glycerol, 1mM DTT, 0.1mM ATP).

Lipids preparation

96% L-α-phosphatidylcholine (EggPC) (Avanti, 840051C) (10 mg/ml in chloroform), 2% DGS-NTA(Ni) (Avanti, 790404C) and 1% DOPE-ATTO390 (ATTO-TEC, 390-161) were mixed into glass tubes, dried with argon gas and incubated under vacuum overnight. The dried lipids were then resuspended in a buffer that we further refer to as the “small unilamellar vesicle (SUV) buffer” (150 mM NaCl, 10mM Tris-HCl pH 7.4 and 2 mM $CaCl_2$) and sonicated on ice for 10 min. The mixture was centrifuged at 20,238 g for 10 min to remove contaminants and the supernatant was collected. The final lipid concentration was 1 mg/ml. For experiments using KIF5B-SNAP-430, unmarked lipids were used (98% EggPC and 2% DGS-NTA(Ni)). Lipids were stored at 4°C for up to a month.

Stabilized microtubules preparation

Unlabeled tubulin (18 µM), Atto-565 tubulin (2 µM) and GMP-CPP (1 mM) were mixed in BRB80 and incubated at 37°C for 2 hours. The mixture was then centrifuged at 20,238 g for 30 min and the microtubules were resuspended in BRB80 supplemented with 10 µM of Taxol. Stabilized microtubules were kept at room temperature for 4 days.

Gliding experiments

Cover glasses and slides were first wiped with lint free tissues and Ethanol 96%, rinsed in ultrapure water, put in Hellmanex III (2% in water, Hellmanex) and sonicated for 30 min at 60°C. The glass was then rinsed in ultrapure water and kept in water for 4 days. We used either flow cell (figure 1, 2A, 3B, 3E, 5A, 5C, S2 and S6) or open well (figure 2B, 2C, 2D, 2E, 3A, 5E and S1) to perform the gliding assays. In both cases the bottom glass coverslip was dried with compressed air, activated with air plasma for 3 min. In the case of open wells, a PDMS square with a punched out 6 mm hole in the center was placed on the glass creating a well. In the case of flow cells, two bands of double-side tape (70 µm height) were covered by a glass corverslip to contain an approximate volume of 15 µl. In both cases, 20 µl of lipids was added, incubated for 10 min then rinsed with SUV buffer. For additional passivation, 1% w/v BSA in HKEM (10 mM HEPES pH=7.2, 50 mM KCl, 1 mM EGTA, 5 mM MgCl2) was incubated for 5 min. BSA was washed out with TicTac buffer (10 mM HEPES buffer (pH 7.2), 16 mM PIPES buffer (pH 6.8), 50 mM KCl, 5 mM MgCl2, 1 mM EGTA, 20 mM dithiothreitol (DTT), 3 mg.ml–1 glucose, 20 µg.ml–1 catalase, 100 µg.ml–1 glucose oxidase, 0.3% BSA) supplemented with 1 mM ATP (Sigma Aldrich, A3377). Motors diluted in TicTac buffer were added and incubated for 5 min, then washed, and microtubules diluted in TicTac buffer were added and incubated for 3 min before being washed as well. Finally, TicTac buffer supplemented with 2.7 mM of ATP and 0.2% methyl cellulose was added prior to imaging. Experiments were performed at room temperature.

Microscopy

Data for Figures 2 and 3A were acquired using an objective-based total internal reflection fluorescence (TIRF) microscopy instrument composed of a Nikon Eclipse Ti, an azimuthal iLas2 TIRF illuminator (Roper Scientific), a ×60 numerical aperture 1.49 TIRF objective lens and an Evolve 512 camera (Photometrics), with 405, 488 and 561 nm lasers (Optical Insights).

Data for Figures 1, 3C and 5E were acquired using an inverted microscope (Ti-E, Nikon), equipped with a total internal reflection fluorescence (TIRF) iLasPulsed system (Gataca Systems) and a Retiga R3 camera (CCD 1920×1460, Binning=1, pixel=4.54 µm) using an Olympus U APO N TIRF oil-immersion 100×1.49 NA objective lens, with a 0.63 O ring.

Data for Figures 5A and 5C were acquired using a Nikon Eclipse Ti2, a 20x objective lens and a Prime BSI-Express camera (pixel=6.5 µm, Binning=2), with 488, 561 and 642 nm lasers.

Multi-stage time-lapse recordings were performed using Metamorph software (version 7.7.5, Universal Imaging) with 100ms of exposure during each acquisition, a time interval of 10 seconds between acquisitions, for a total duration of 30 to 60 minutes.

FRAP experiments

Experiments were done on an inverted microscope (Ti-E, Nikon), equipped with a total internal reflection fluorescence (TIRF) iLasPulsed system (Gataca Systems) and a Retiga R3 camera (CCD 1920x1460, Binning = 2, 6.93 pixels per micron) using an Olympus U APO N TIRF oil-immersion 100x 1.49 N.A. objective lens, with a 0.63 O ring. FRAPs were performed in rectangular regions of 60X40 pixels at 100% laser power with 1119 ms in the 642 nm channel and 872 ms exposure time in the 491 nm channel for KIF5B and NCD respectively. For the Movie S4, a bigger region of 60X400 pixels were frapped in both the channels at the same time with 100% laser power. The images were acquired with a time interval of 10 seconds each for 5 minutes.

Laser ablation experiments

Experiments were done on a confocal spinning disk microscope (Nikon Ti Eclipse equipped with a spinning scanning unit CSU-X1 Yokogawa) and a R3 retiga camera (QImaging). Images were acquired using a Nikon CFI Super Fluor 100x/1.3 NA oil objective. Each wavelength was acquired separately. Photoablation was performed using the iLas2 device (Gataca Systems) equipped with a passively Q-switched laser (STV-E,ReamPhotonics) at 355 nm producing 500 picosecond pulses. Laser displacements, exposure time and repetition rate were controlled via the ILas software interfaced with MetaMorph (Universal Imaging Corporation). Laser photoablation and subsequent imaging were performed with a CFI Super Fluor 100X/1.3 NA oil objective. The ablations were performed along a single curve whose width was defined to be 10 pixels for the microtubule destruction and 4 pixels for the local microtubule severing. The laser parameters used to cut microtubules were the following : laser power was set to 40% with a total of 8 repetitions.

Microtubule tracking

Tracking was performed using a custom-made Python3 script, based on previous work (*6*). Briefly, the contours of a microtubule are identified in binarized TIRF images, its center **r** is found and two contours in successive frames are considered part of the same trajectory if they are close enough and no other contour is closer. Additionally, contours can be part of the same trajectory only if their orientation and size did not change significantly (<40 %). The velocity is computed as $\mathbf{v}=[\mathbf{r}(t+dt)-\mathbf{r}(t)]/dt$. As a final check, the angle between v and the orientation of the contour has to be smaller than 36. The histogram of $|\mathbf{v}|$ is used to compute the mean speed.

Motor domains size measurement

To analyze the size of the patterns and area fractions over time, we start from microscopy images (20x, epifluorescence), using the NCD or KIF5B channel separately. The images are binarized manually so that only the parts of the image containing NCD or KIF5B patterns are above threshold, both in the gliding and in the pattern phase. The area fraction is computed as the number of pixels above threshold divided by the number of pixels in the image. An area fraction of 1 corresponds to gliding (motors everywhere uniformly) while an area fraction of 0 corresponds to the absence of motors of a given kind. Intermediate values indicate accumulation of motors in parts of the image, i.e. patterns. Notice that because the two channels are analyzed separately, and because of

accumulation of motors on the MTs, the sum of the area fractions of the two motors is not imposed to be 1.

Motors density measurement

In Figure 1, the motors' profile was obtained by imaging almost-immobile microtubules in a tug-of-war condition at [NCD]=2 nM and [KIF5B]=0.6 nM for 10 minutes with a time interval of 3s. In Figure S3 the motors' profile was obtained by imaging patterns generated by the self-organization of microtubules in a dense array forming a boundary between motor domains in response to [NCD]=36 nM and [KIF5B]=7 nM for 10 minutes with a time interval of 3s. The image series were averaged and a line scan along the microtubule was performed with Fiji to obtain the motor profile on one microtubule. Several profiles were then selected, oriented so that the maximum of NCD is on the same side and finally averaged together to obtain the mean profile. Profiles are then compared with a plot of Equation 21 (see Supplementary Text), where one of the two profiles is mirrored as it goes from x=l to x=0.

Supplementary References

1. M. Vantard, C. Peter, A. Fellous, P. Schellenbaum, A. M. Lambert, Characterization of a 100-kDa heat-stable microtubule-associated protein from higher plants. *Fed. Eur. Biochem. Soc. J.* **220**, 847–853 (1994).

2. M. L. Shelanski, Chemistry of the filaments and tubules of brain. *J. Histochem. Cytochem.* **21**, 529–39 (1973).

3. A. Hyman, D. Drechsel, D. Kellogg, S. Salser, K. Sawin, P. Steffen, L. Wordeman, T. J. Mitchison, Preparation of modified tubulins. *Methods Enzymol.* **196**, 478–485 (1991).

4. R. B. Case, D. W. Pierce, N. Hom-Booher, C. L. Hart, R. D. Vale, The directional preference of kinesin motors is specified by an element outside of the motor catalytic domain. *Cell*. **90**, 959–966 (1997).

5. T. Korten, S. Chaudhuri, E. Tavkin, M. Braun, S. Diez, Kinesin-1 Expressed in Insect Cells Improves Microtubule in Vitro Gliding Performance, Long-Term Stability and Guiding Efficiency in Nanostructures. *IEEE Trans. Nanobioscience*. **15**, 62–69 (2016).

6. A. Sciortino, L. J. Neumann, T. Krüger, I. Maryshev, T. F. Teshima, B. Wolfrum, E. Frey, A. R. Bausch, Polarity and chirality control of an active fluid by passive nematic defects. *Nat. Mater.* **22**, 260–268 (2023).

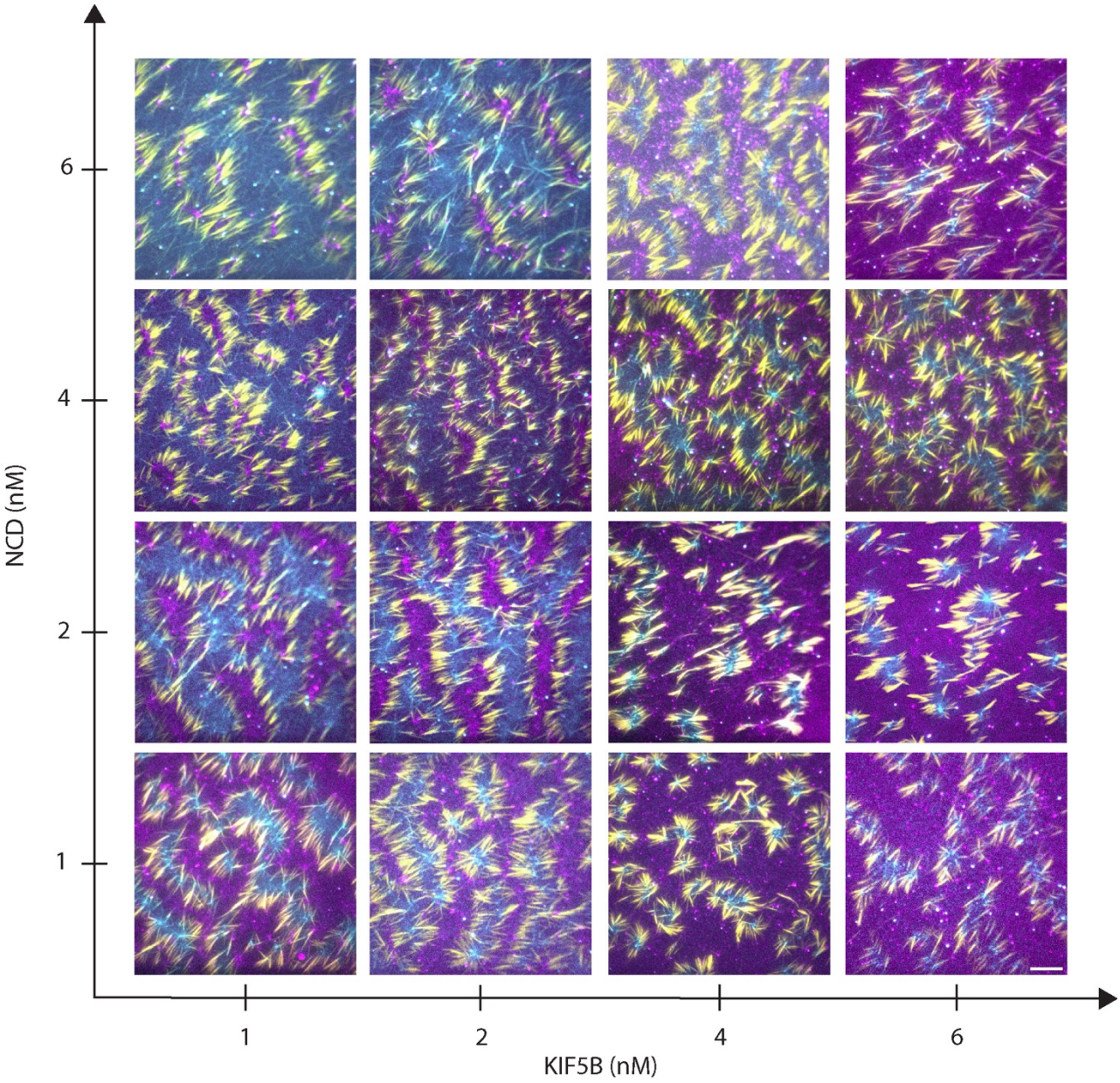

Figure S1. Different examples of pattern formation.

Microscopy imaging of microtubules (yellow) and motors (KIF5B in magenta, NCD in cyan) at varying motor concentrations (scale bar: 20 µm).

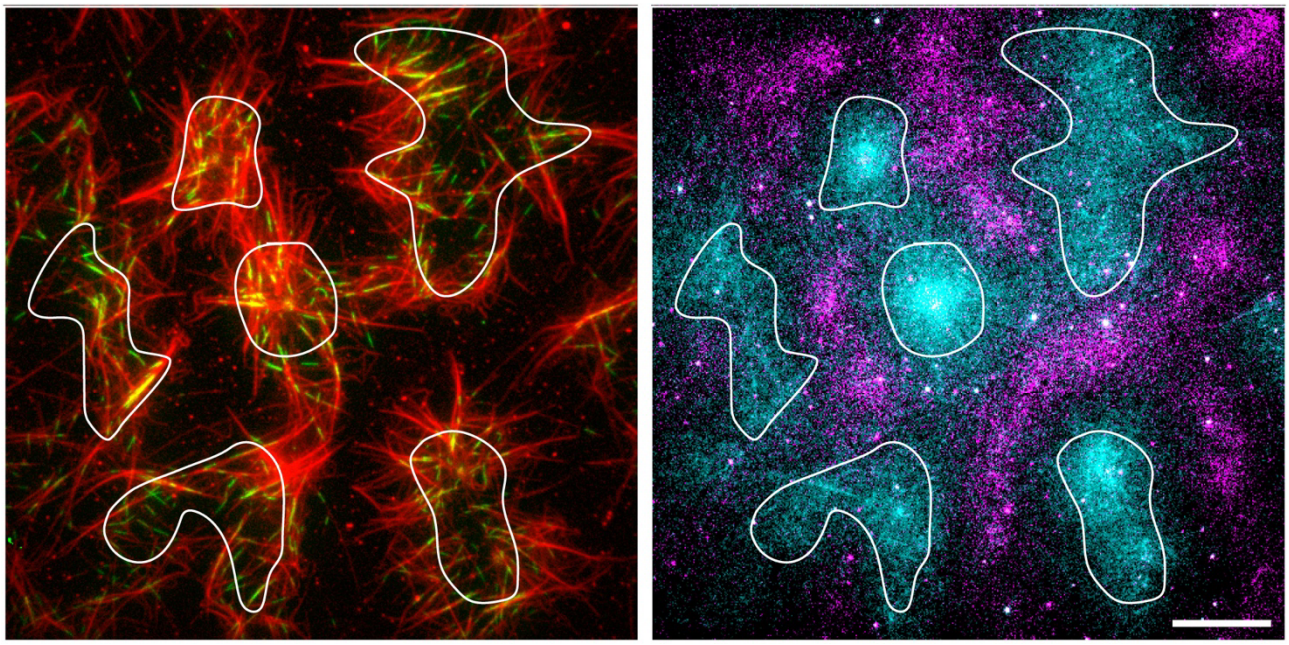

Figure S2. Motor segregation sorted microtubules based on their polarity.

These images show the sorting of dynamic microtubules (red) assembled from stabilized seeds (green) which therefore marked microtubules minus ends. Plus-end directed motors (KIF5B, magenta) and minus-end directed motors (NCD, cyan) were segregated by their directed walk. As they walk, motors moved microtubules which became sorted based on their polarity. Eventually, microtubule minus-ends (green) were localized in domains were minus-end directed motors were segregated (cyan, surrounded by a white contour to facilitate visual comparison with the localization of microtubule minus-ends). Scale bar represents 20 micrometers.

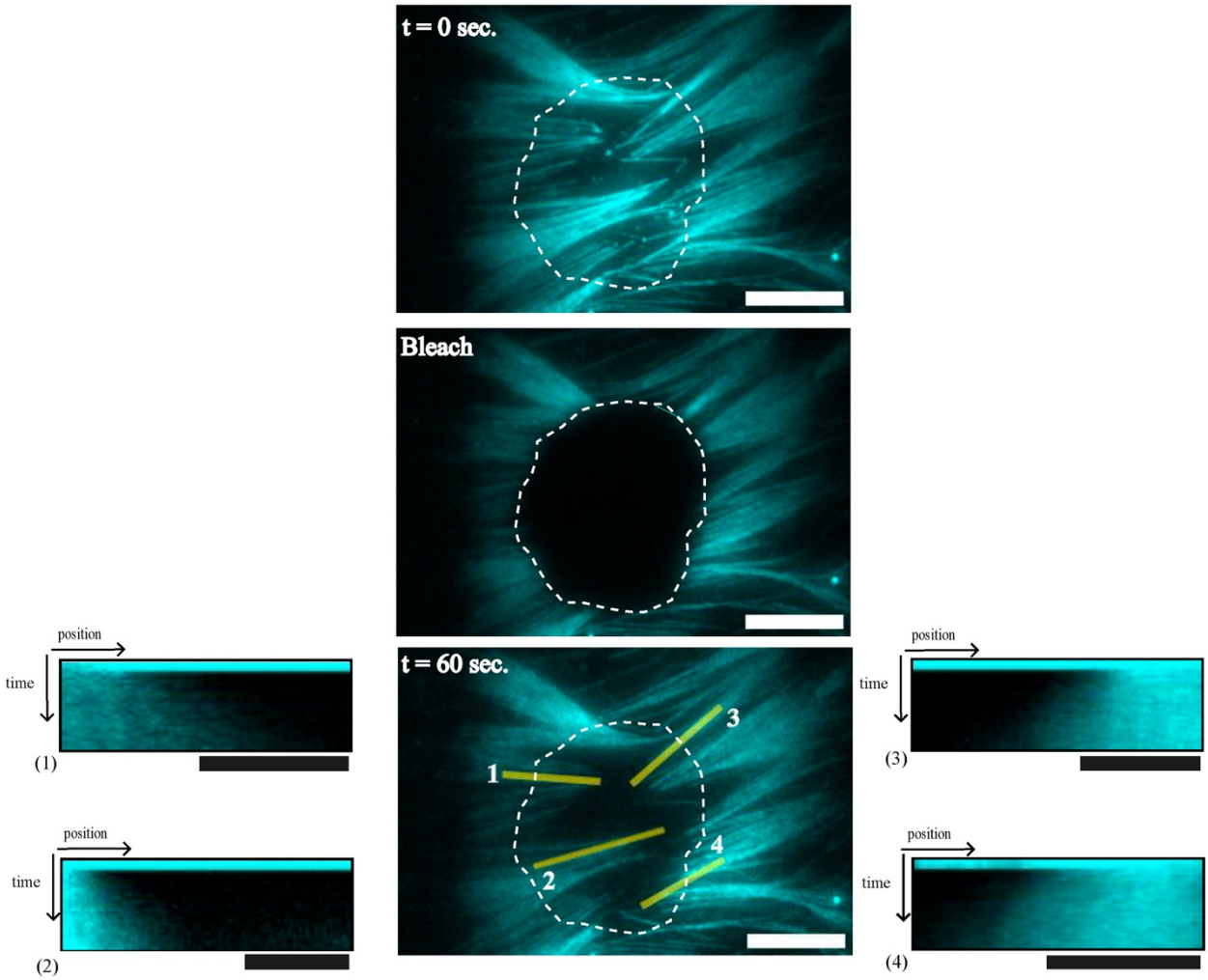

Figure S3. FRAP of motors along microtubules

Photo-bleaching of NCD motors along microtubules forming domains where NCD was the concentrated in the inner domain. Only a section of the microtubule was bleached. We then monitored signal recovery for 60 seconds. Supplementary movie S5 clearly showed that the motor fluorescence from the non-bleached region moved radially along the microtubules toward the central domain. This could also be highlighted by the evolution of fluorescence during the first 15 seconds along linescans as shown by the kymographs displayed on the side of the central image. Scale bars represent 10 μm.

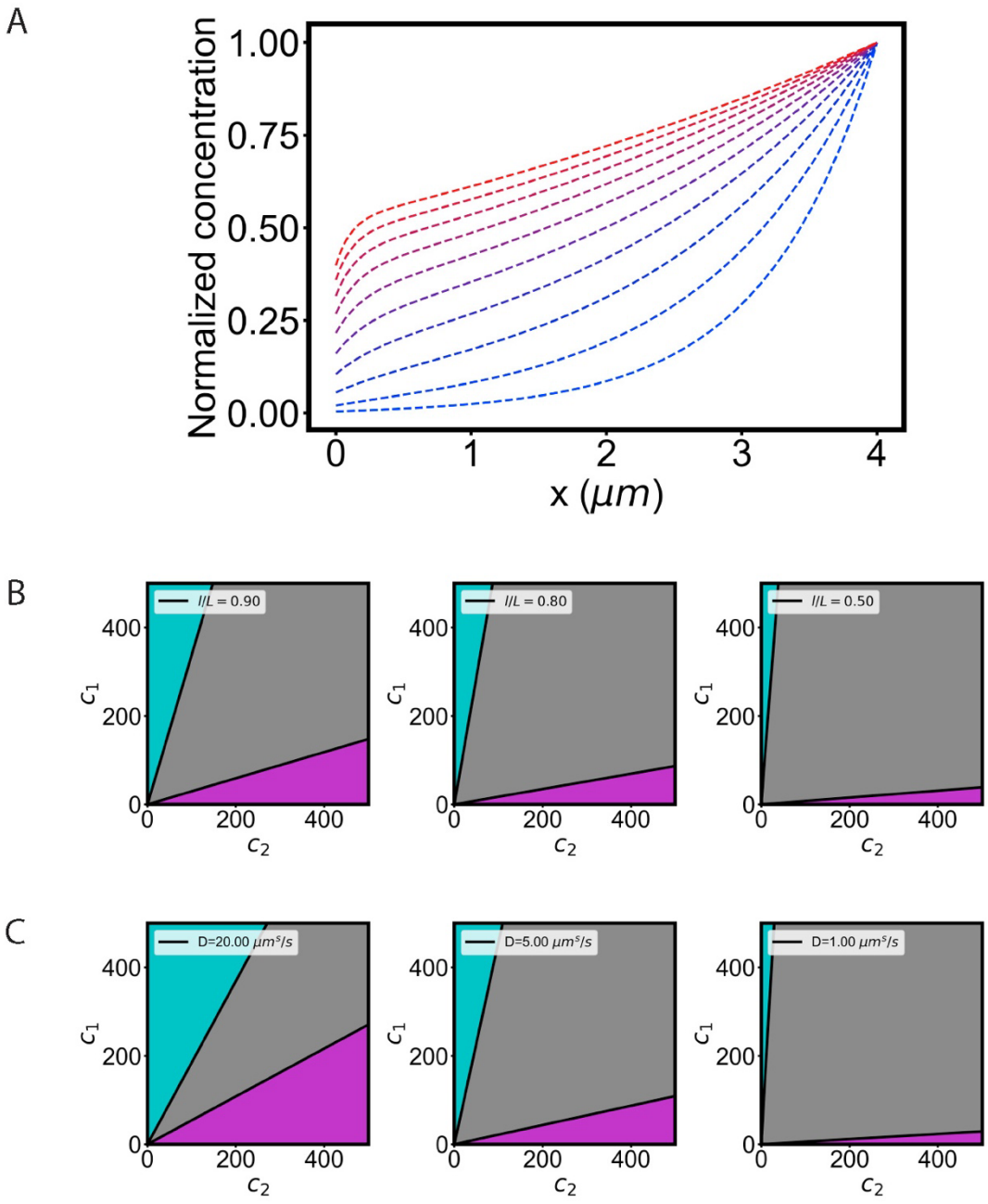

Figure S4. Theoretical prediction of phase diagram evolution.

(A) Plot of normalized concentration of motors, C_{tot}/C_{max} (C_{max} refers to the maximum concentration for the given parameters), along the length of microtubule x is shown. We plot the data for k_{off} = [0, 10], and the color bar from blue to red refers to the increase of k_{off}. We keep all other parameters fixed, diffusion constant D = 2.0 μm^2/sec, speed of the motors v = 1 μm/sec, k_{on} = 3.0 sec^{-1}, domain size L = 20 μm, average length of microtubule l = 4.0 μm, and c_m = 10 motors/μm. **(B)** Phase diagrams for different microtubule lengths. **(C)** Phase diagrams for different diffusion coefficients.

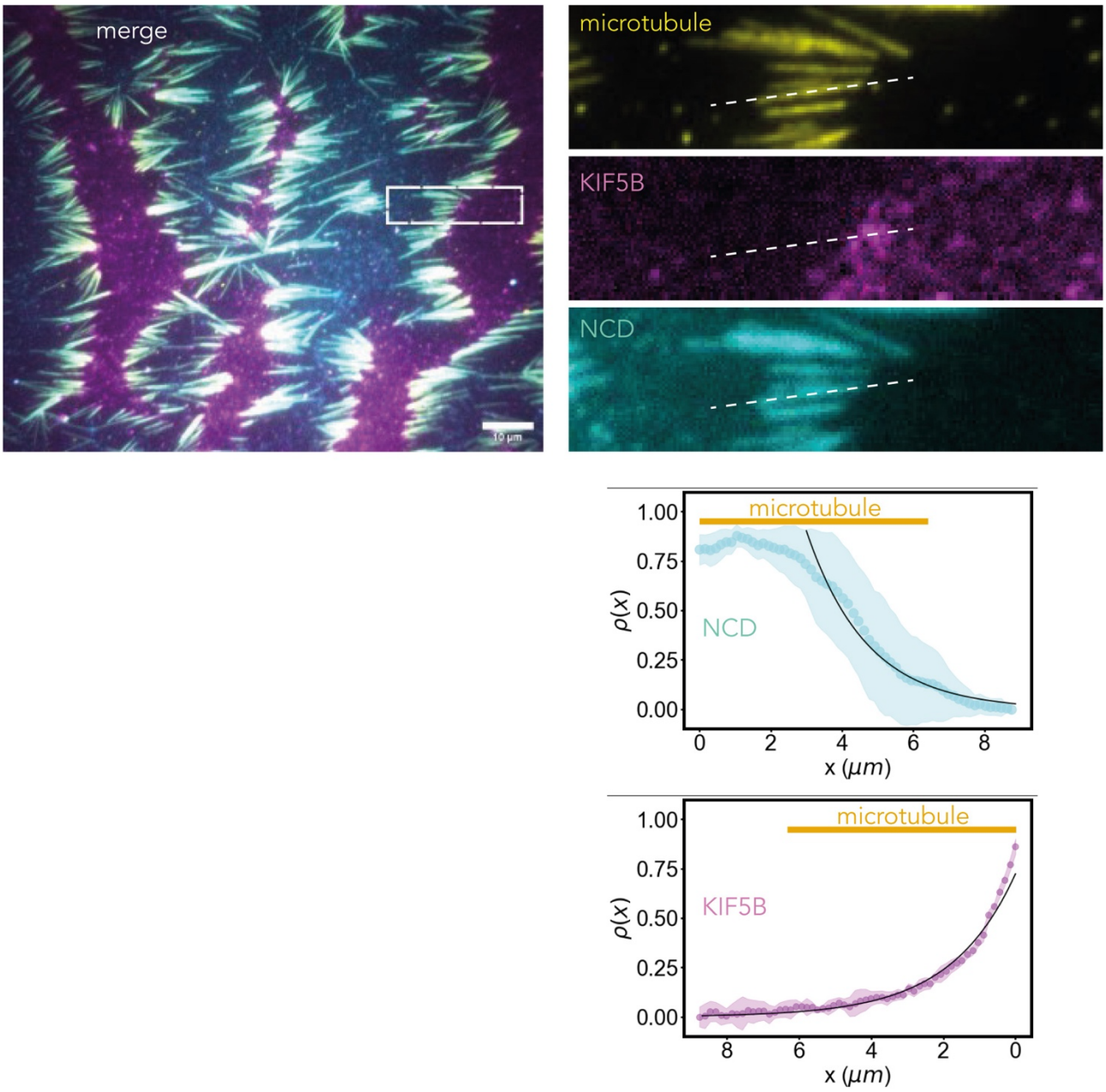

Figure S5. Theoretical prediction and experimental measurements of motors concentration under individual microtubule forming active boundaries between motor domains.

Images show stabilized microtubles and motors self-organization in the presence of 4nM of KIF5B and 4 nM of NCD Scale bar represents 10 micrometers. Dashed lines illustrate the linescans that were performed to measure the linear densities, ρ, of motors. Microtubules of various length were aligned to their minus-ends to measure NCD linear densities, and to their plus-ends to measure KIF5B linear densities. Graphs show the experimental measurements of motor density profiles and the black curves show the theoretical prediction of these densities according to our model using D=0.3 $\mu m^2/s$, and k_{on}=3.0 s-1, k_{off}=2.5 s^{-1}, v=0.5 µm/s for KIF5B, and k_{on}=6.0 s-1, k_{off}=14 s^{-1}, v=0.2 µm/s for NCD.

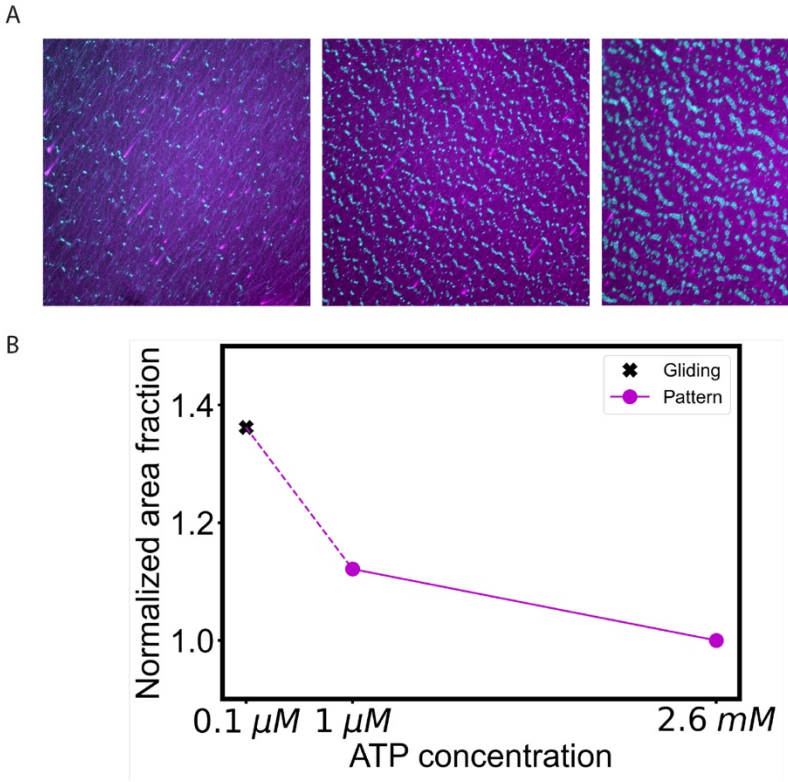

Figure S6. Transition between gliding and self-patterning states and variations of pattern size in response to modulations of ATP concentration.

(A) Microscopy imaging of KIF5B and NCD for three ATP concentrations: 0.1 µM, 1 µM and 2.6 mM (scale bar: 50 µm). **(B)** Normalized area fraction of KIF5B for the three ATP concentrations.

Supplementary Movies

Movie S1. **Microtubule gliding.**

Microscopy imaging of microtubules at low density gliding on KIF5B, NCD and both motors. Data is also shown in Figure 1B. Movie duration is 10 min and it is compressed in JPEG at 20 frames per second.

Movie S2. Microtubule alignment and bundling.

Microscopy imaging of microtubules gliding on opposite motors and bundling upon contact. Data is also shown in Figure 2A. Movie duration is 26 min and it is compressed in JPEG at 30 frames per second.

Movie S3. Microtubules and motors self-patterning.

Microscopy imaging of microtubules (yellow), NCD (cyan) and KIF5B (magenta), at high microtubule density, self-organizing into patterns. Data is also shown in Figure 3A. Movie duration is 60 min and it was compressed in JPEG at 30 frames per second.

Movie S4. **Microtubules and motors turnover in self-patterned domains.**

Microscopy imaging of microtubules on the left, and NCD (cyan) and KIF5B (magenta) on the right, during a photo-bleaching and FRAP experiment where the three proteins fluorescent signals are extinguished. Movie duration is min 20 sec and it is compressed in JPEG at 20 frames per second.

Movie S5. **Motors transport in self-patterned domains.**

Microscopy imaging of NCD (cyan) motors during a photo-bleaching and FRAP experiment. Movie duration is 1 min 20 sec and it is compressed in JPEG at 20 frames per second.

Movie S6. Patterns dissolution by partial microtubule destruction.

Microscopy imaging of microtubules (yellow), NCD (cyan) and KIF5B (magenta) during a laser ablation experiment where an entire microtubule band is destroyed on the side of the pattern. Movie duration is 22 min and it is compressed in JPEG at 20 frames per second.

Movie S7. Microtubule severing

Microscopy imaging of microtubules (yellow), NCD (cyan) and KIF5B (magenta) during a laser ablation experiment, where microtubules on the side of a pattern are cut in the middle. Data is shown in Figure 3E. Movie duration is 8 min 20 sec and it is compressed in JPEG at 20 frames per second.

Movie S8. Transition between gliding and self-patterning states.

Microscopy imaging of microtubules (yellow), NCD (cyan) and KIF5B (magenta) going from NCD gliding to patterns after KIF5B addition, and finally to KIF5B gliding after a second KIF5B addition. Data is also shown in Figure 5E. Movie duration is 83 min and it is compressed in JPEG at 30 frames per second.